

H. C. Weiss, D. Bläser, R. Boese, A. Nangia, G. R. Desiraju, *J. Am. Chem. Soc.* **1998**, *120*, 8702; c) For further details, see: <http://www.ohcd-system.com>.

- [8] Crystal structure analyses: The data were collected at 130 K either on a Nicolet R3 or on a SMART diffractometer using Mo α radiation. The data were corrected for cylindrical shape for crystals grown in situ. Structure solution by direct methods and refinements on F^2 with SHELXL-Plus (Version 5.03). All non-hydrogen atoms were refined anisotropically. The positions of the hydrogen atoms were taken from a difference Fourier map and refined isotropically without constraints. a) 1,3-Propanediol: space group $P2_1/n$, $2\theta_{\max} = 60^\circ$, reflections measured: 1255, independent: 1200, observed ($I > 2\sigma_I$): 951, 78 parameters, $R1 = 0.046$, $wR2 = 0.153$, residual electron density $+0.39/-0.20 \text{ e \AA}^{-3}$ (CCDC-132862); b) 1,4-butanediol: space group $P2_1/n$, $2\theta_{\max} = 55^\circ$, reflections measured: 2432, independent: 1134, observed ($I > 2\sigma_I$): 964, 95 parameters, $R1 = 0.063$, $wR2 = 0.164$, residual electron density $+0.45/-0.51 \text{ e \AA}^{-3}$ (CCDC-132863); c) 1,5-pentanediol: space group $P2_12_12_1$, $2\theta_{\max} = 60^\circ$, reflections measured: 3628, independent: 1774, observed ($I > 2\sigma_I$): 1632, 112 parameters, $R1 = 0.031$, $wR2 = 0.084$, residual electron density $+0.26/-0.17 \text{ e \AA}^{-3}$ (CCDC-132864); d) 1,6-hexanediol: space group $P2_1/n$, $2\theta_{\max} = 60^\circ$, reflections measured: 1455, independent: 1206, observed ($I > 2\sigma_I$): 911, 129 parameters, $R1 = 0.045$, $wR2 = 0.134$, residual electron density $+0.26/-0.22 \text{ e \AA}^{-3}$ (CCDC-132865); e) 1,7-heptanediol: space group $P2_12_12_1$, $2\theta_{\max} = 60^\circ$, reflections measured: 1908, independent: 1883, observed ($I > 2\sigma_I$): 1313, 144 parameters, $R1 = 0.058$, $wR2 = 0.151$, residual electron density $+0.24/-0.28 \text{ e \AA}^{-3}$ (CCDC-132866); f) 1,8-octanediol: space group $P2_1/n$, $2\theta_{\max} = 60^\circ$, reflections measured: 3510, independent: 1248, observed ($I > 2\sigma_I$): 1084, 82 parameters, $R1 = 0.036$, $wR2 = 0.097$, residual electron density $+0.33/-0.22 \text{ e \AA}^{-3}$ (CCDC-132867); g) 1,9-nonanediol: space group $P2_12_12_1$, $2\theta_{\max} = 60^\circ$, reflections measured: 3544, independent: 2603, observed ($I > 2\sigma_I$): 1357, 180 parameters, $R1 = 0.072$, $wR2 = 0.158$, residual electron density $+0.47/-0.22 \text{ e \AA}^{-3}$ (CCDC-132868); h) 1,2-ethanediamine: space group $P2_1/c$, $2\theta_{\max} = 60^\circ$, reflections measured: 1614, independent: 520, observed ($I > 2\sigma_I$): 477, 35 parameters, $R1 = 0.065$, $wR2 = 0.166$, residual electron density $+0.78/-0.45 \text{ e \AA}^{-3}$ (CCDC-132869); i) 1,3-propanediamine: space group $Cmc2_1$, $2\theta_{\max} = 60^\circ$, reflections measured: 1504, independent: 502, observed ($I > 2\sigma_I$): 477, 47 parameters, $R1 = 0.032$, $wR2 = 0.082$, residual electron density $+0.19/-0.28 \text{ e \AA}^{-3}$ (CCDC-132870); j) 1,4-butanediamine: space group $Pbca$, $2\theta_{\max} = 60^\circ$, reflections measured: 3172, independent: 794, observed ($I > 2\sigma_I$): 745, 52 parameters, $R1 = 0.042$, $wR2 = 0.120$, residual electron density $+0.23/-0.26 \text{ e \AA}^{-3}$ (CCDC-132871); k) 1,5-pentanediamine: space group $Cmc2_1$, $2\theta_{\max} = 60^\circ$, reflections measured: 3600, independent: 972, observed ($I > 2\sigma_I$): 892, 64 parameters, $R1 = 0.039$, $wR2 = 0.104$, residual electron density $+0.24/-0.24 \text{ e \AA}^{-3}$ (CCDC-132872); l) 1,6-hexanediamine: space group $Pbca$, $2\theta_{\max} = 60^\circ$, reflections measured: 1249, independent: 1069, observed ($I > 2\sigma_I$): 899, 69 parameters, $R1 = 0.061$, $wR2 = 0.177$, residual electron density $+0.55/-0.31 \text{ e \AA}^{-3}$ (CCDC-132873); m) 1,7-heptanediamine: space group $Cmc2_1$, $2\theta_{\max} = 60^\circ$, reflections measured: 3114, independent: 1159, observed ($I > 2\sigma_I$): 1067, 81 parameters, $R1 = 0.032$, $wR2 = 0.095$, residual electron density $+0.36/-0.17 \text{ e \AA}^{-3}$ (CCDC-132874); n) 1,8-octanediamine: space group $Pbca$, $2\theta_{\max} = 45^\circ$, reflections measured: 1098, independent: 593, observed ($I > 2\sigma_I$): 449, 86 parameters, $R1 = 0.031$, $wR2 = 0.084$, residual electron density $+0.08/-0.14 \text{ e \AA}^{-3}$ (CCDC-132875). Crystallographic data (excluding structure factors) for the structures reported in this paper have been deposited with the Cambridge Crystallographic Data Centre as supplementary publication nos. CCDC-132862 to CCDC-132874. Copies of the data can be obtained free of charge on application to CCDC, 12 Union Road, Cambridge CB2 1EZ, UK (fax: (+44) 1223-336-033; e-mail: deposit@ccdc.cam.ac.uk).
- [9] The crystal structures of some of the compounds studied here have been reported. The analyses were carried out at different temperatures and sometimes to lower accuracies: a) 1,2-ethanediol at 130 K: R. Boese, H. C. Weiss, *Acta Crystallogr. Sect. C* **1998**, *54*, 24; b) 1,6-hexanediol at 300 K: M. Lindgren, T. Gustafsson, J. Westerling, A. Lund, *Chem. Phys.* **1986**, *106*, 441; c) 1,9-nonanediol and 1,10-decanediol at 100 K: ref. [2g]; d) 1,2-ethanediamine at 210 K: S. Jamet-Delcroix, *Acta Crystallogr. Sect. B* **1973**, *29*, 977; e) 1,6-

hexanediamine at 300 K: W. P. Binnie, J. M. Robertson, *Acta Crystallogr.* **1950**, *3*, 424; f) 1,7-heptanediamine at 210 K: R. Gotthardt, J. H. Fuhrhop, J. Buschmann, P. Luger, *Acta Crystallogr. Sect. C* **1997**, *53*, 1715.

- [10] C. P. Brock, L. L. Duncan, *Chem. Mater.* **1994**, *6*, 1307.
 [11] V. R. Thalladi, H.-C. Weiss, R. Boese, A. Nangia, G. R. Desiraju, *Acta Crystallogr. Sect. B* **1999**, *55*, 1005, and references therein.
 [12] The geometries of the O–H...O bonds are similar at the two ends of the molecules, which also holds for C4 and C6-diols where $Z' = 1$.
 [13] This is further corroborated by the fact that the calculated packing fractions for even diols and even diamines are systematically higher than those for the corresponding odd members (Table 1) and exhibit an alternating trend similar to that of the melting points and densities.
 [14] We have used the Dreiding-II force field built-in the crystal packer module of the Cerius² program. All calculations were performed as the snapshots of crystal structures. The overall result is the same even after the crystal structures were minimized.
 [15] One of the C–O groups adopts a strained *gauche* conformation in odd diols in the solid state, which also contributes to the lowering of the melting points of odd diols.
 [16] Increased hydrophobicity does not alter the structural patterns in diols. Higher analogues of even and odd diols (a) 1,11-undecanediol: N. Nakamura, S. Setodoi, T. Ikeya, *Acta Crystallogr. Sect. C* **1999**, *55*, 789; b) 1,12-dodecanediol: N. Nakamura, S. Setodoi, *Acta Crystallogr. Sect. C* **1997**, *53*, 1883; c) 1,13-tridecanediol: N. Nakamura, Y. Tanihara, T. Takayama, *Acta Crystallogr. Sect. C* **1997**, *53*, 253; d) 1,16-hexadecanediol: N. Nakamura, T. Yamamoto, *Acta Crystallogr. Sect. C* **1994**, *50*, 946) adopt structures isomorphous to their lower analogues.

Bridged Cyclic Oligoribonucleotides as Model Compounds for Codon–Anticodon Pairing**

Ronald Micura,* Werner Pils, and Karl Grubmayr

Dedicated to Professor Albert Eschenmoser on the occasion of his 75th birthday

The base sequences of genes are translated with complementary mRNA and the assistance of tRNAs into protein sequences. This process takes place at the ribosome.^[1] Thereby, the formation of specific Watson–Crick base pairs between codon (mRNA) and anticodon (tRNA) is crucial. The structure of the corresponding pairing complex is similar to a double helical A-form RNA.^[2, 3] Although in general,

[*] Dr. R. Micura,^[+] Dipl.-Ing. W. Pils, a. Univ.-Prof. Dr. K. Grubmayr Institut für Chemie Johannes Kepler Universität Linz Altenbergerstrasse 69, 4040 Linz (Austria) Fax: (+43) 732-2468-747 E-mail: micura@gmx.net

[+] Alternative address: Laboratorium für Organische Chemie der Eidgenössischen Technischen Hochschule Universitätstrasse 16, 8092 Zürich (Switzerland) Fax: (+41) 1-632-1043

[**] R.M. acknowledges the Austrian Academy of Science for an APART fellowship (Austrian Programme for Advanced Research and Technology). This work was supported by the Austrian Science Fund, Vienna (P13216-CHE). R.M. is obliged to Prof. Eschenmoser (Zürich) and Prof. Falk (Linz) for generous hospitality in their laboratories. We thank Dr. Krishnamurthy (Scripps Institute, La Jolla, California) for mass analyses and Dr. Weiss (Xeragon AG, Zürich) for 2'-O-TOM-phosphoramidites of standard bases.

complementary oligoribonucleotides in aqueous buffer solutions acquire such a geometry, a duplex consisting of solely three base pairs is too weak to allow determination of its pairing properties through routine UV and CD spectroscopic methods.^[4] The development of new model compounds with increased three base pair duplex stabilities is the aim of the work presented here. In particular, stacking interactions which are known, or assumed to be, of significance during codon–anticodon pairing are taken into account.

We based the modeling of a codon–anticodon pairing complex on the crystal structure of a tRNA which codes for phenylalanine^[5] and on the assumption of A-type helix formation with respect to the codon–anticodon interaction (Figure 1).^[2–4] With regard to the stereochemical situation it can be deduced that a structurally related model must not be restricted to the three base pairs themselves. The modified purine base 37 at the 3'-end of the anticodon propagates the A-form helix and ideally interferes with the first base pair of the codon–anticodon core duplex by base stacking. In a comparable manner, base stacking is conceivable at the opposite end of the helix which comprises the base at the 3'-end of the codon.^[6] In contrast, the bases which are attached to the core duplex through the 5'-end are unable to interfere by base stacking.

According to the structural features described above, two types of chemical constitutions (**I** and **II**) are justifiable as appropriate model compounds. They also fit the criteria described for the different pairing modes of tRNA and mRNA within the P-Site and the A-Site of the ribosome.^[2, 3] Both types **I** and **II** contain 1-methylguanosine (*m¹G*) as the representative for the modified tRNA purine bases at position 37^[7] and, optionally, in model compounds of type **II**, the first base of the following codon is taken into account (Figure 2). The characteristic structural feature of the model compounds is the covalent bridging of short complementary nucleotide sequences by hexa- or heptaethylene glycol units.^[8] The linkage spans from a 5'-phosphate group to the corresponding opposite 3'-phosphate group of the ribose backbone and, therefore, does not directly affect base pairing.

In accordance with the modeling we chose an anticodon sequence motif of tRNA which codes for phenylalanine, namely 5'-GAAM¹G,^[9] and synthesized the macrocycles **1–7** (shown in Table 1) following a solid-phase approach which was developed for the preparation of cyclic oligoribonucleotides in general.^[10] All compounds were characterized by MALDI-TOF mass spectrometry and their pairing properties investigated.

The temperature-dependent trace of UV absorption at 265 nm shows sigmoid melting profiles for the macrocycles **1–7** in aqueous buffer systems (Figure 3). The corresponding melting transitions are independent of concentration and are observed in a temperature region that guarantees a reliable determination of thermodynamic parameters.^[11] The stability

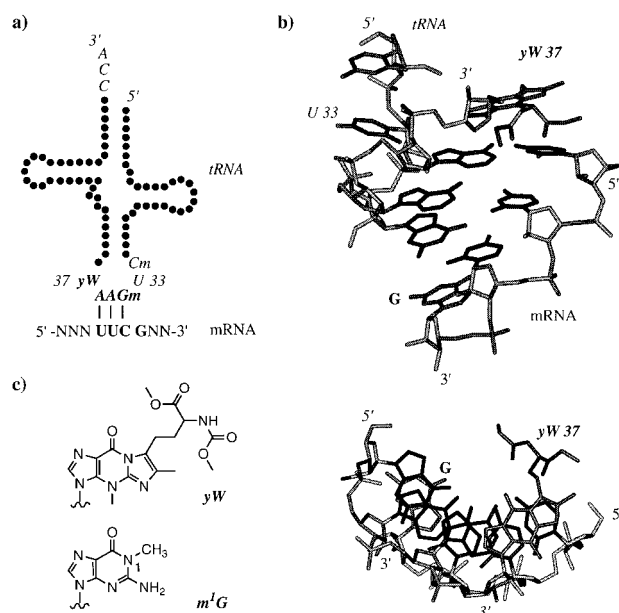


Figure 1. Codon–anticodon pairing of tRNA^{Phe} from *Saccharomyces cerevisiae* (tRNA symbols in *italic* style). a) Sequence motif: wybutosine (yW), 2'-*O*-methylguanosine (Gm), 2'-*O*-methylcytosine (Cm). b) Modeling: views perpendicular (above) and parallel (below) to the helix axis; the nonpairing bases wybutosine (tRNA) and guanosine (mRNA) at the 3'-ends of the codon–anticodon duplex interfere by base stacking. c) Structural formula of tRNA^{Phe} purine bases at position 37; 1-methylguanosine (*m¹G*).^[3, 5]

of the minihelices is of entropic origin and is displayed in the high absolute values of the entropic terms which reach up to 100 cal mol⁻¹ K⁻¹ (Table 1).

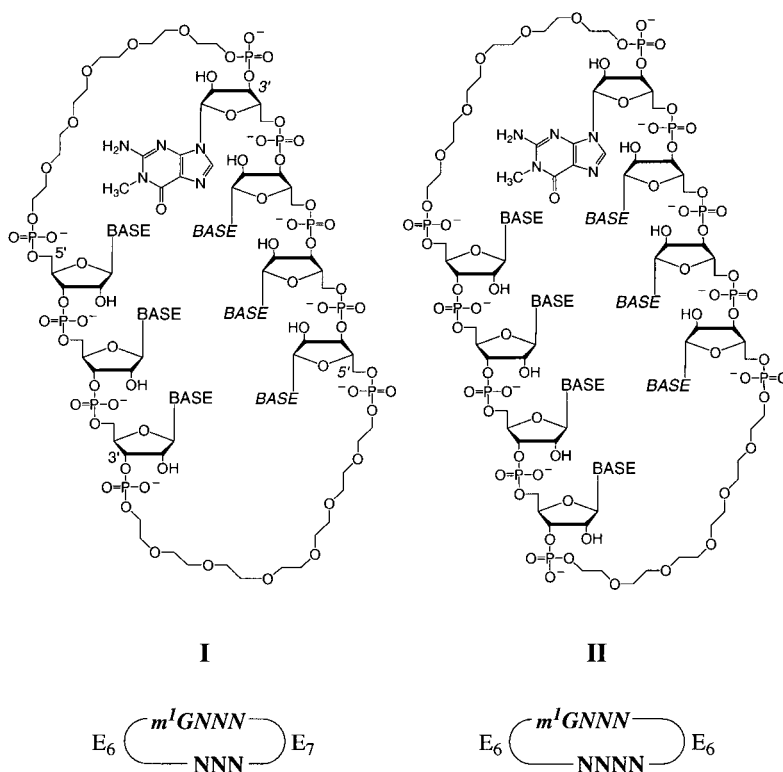


Figure 2. Constitutional types **I** and **II** of cyclic model compounds for the codon–anticodon pairing. N, N = nucleotides, E₆ = hexaethylene glycol phosphate, E₇ = heptaethylene glycol phosphate.

Table 1. Selected cyclic oligoribonucleotides containing the sequence motif of the tRNA^{Phe} codon–anticodon pairing.

Constitution type	No.	Base sequence	T_m ^[a] [°C]	ΔH° ^[c] [kcal mol ⁻¹]	Thermodynamic data ^[b]		MALDI-TOF-MS	
					ΔS° ^[c] [cal mol ⁻¹ K ⁻¹]	ΔG_{298}° [kcal mol ⁻¹]	[M+H] ⁺ (theor.)	[M+H] ⁺ (obs.)
I	1	E ₇ (AAG/UUC) E ₇	36.0	-22.7 (-19.3)	-73.4 (-51.5)	-0.8	2698	2698
	2	E ₆ (GAAG/UUC) E ₇	41.2	-26.8 (-24.8)	-85.3 (-66.5)	-1.4	2999	2999
	3	E ₆ (m ¹ GAAG/UUC) E ₇	42.6	-27.6	-87.4	-1.5	3013	3011
II	4	E ₆ (m ¹ GAAG/UUCG) E ₆	49.9	-33.3	-103.1	-2.6	3314	3313
II	5	E ₆ (m ¹ GAAG/UUCU) E ₆	43.8	-30.1	-95.3	-1.7	3275	3276
II	6	E ₆ (m ¹ GAAG/UUUG) E ₆	18.0	-17.8	-61.1	+0.4	3315	3316
II	7	E ₆ (m ¹ GAAG/UUUU) E ₆	16.5	-16.1	-55.6	+0.5	3276	3278

[a] Melting temperatures T_m : 4 μ M, 1.0M NaCl, 0.01M Na₂HPO₄, pH 7.0. [b] Determination of ΔH° and ΔS° from plots of α against T . See ref. [11] and ref. [12], p. 1119. The analysis by differentiation of the melting profiles according to ref. [11a], p. 1610 gave similar values. [c] The terms in brackets provide the ΔH° and ΔS° contributions within a (bimolecular) duplex calculated on the basis of free-energy parameters tabulated for single standard base pairs. See ref. [11b], p. 30, p. 34.

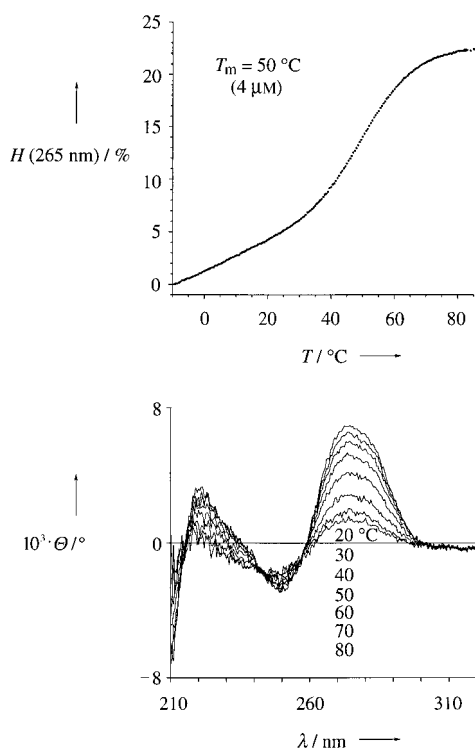


Figure 3. Temperature dependence of the base pairing of cy-rGAAm¹G-E₆-UUCG-E₆ **4** (4 μ M, 1.0M NaCl, 0.01M Na₂HPO₄, pH 7). Above: UV melting profile. Below: CD spectra. H = hyperchromicity, $\Delta T = 0.7$ K min⁻¹.

The comparison of the thermodynamic stabilities of pairing complexes that belong to the different constitutional types **I** and **II** is reasonable despite their different ring size. A detailed study concerning this matter suggests that differences in stability which originate from conformational changes of the linkers or from different linker lengths are small when compared to the stabilization which arises from base stacking

by an additionally attached nucleotide.^[8] Therefore, it can be outlined that the pairing complex which consists of the three base pairs UUC/GAA is significantly stabilized by nonpairing, dangling bases at one or both 3'-ends (Table 1; **1–5**). In general, the extent of stabilization is higher with purine bases than pyrimidine bases (Table 1; **4, 6** compared with **5, 7**). This might be of interest with respect to evolution of tRNA structures as tRNA bases at position 37 are, without exception, of purinic structure. Moreover, their chemical modifications often enable additional interstrand stacking and, therefore, potentially enhance duplex stabilities. In nature, these principles seem to be best realized in the tricyclic base wybutosine (Figure 1),^[13] however even the frequently occurring 1-methylguanosine causes a definite stabilization of our model compounds compared to the unmodified guanosine (Table 1; **3** compared with **2**).

1-Methylguanosine has another characteristic feature in common with modified tRNA bases at position 37: its 1-methyl group hampers base pairing according to the Watson–Crick mode. For compound **7**, this property is the reason for retaining the reading frame of UUU/GAA; the incorporation of guanosine instead of 1-methylguanosine would most likely cause slippage from the intended pairing complex of three base pairs towards one consisting of the corresponding four base pairs.^[14]

This principle of cyclic bridging through flexible linkers offers the availability of very short, but highly stable, double helical RNAs. The physico chemical and structural properties of these compounds can be easily ascertained with standard methods used in the field of oligonucleotide chemistry. In particular, double helices of three base pairs represent model compounds for codon–anticodon interactions and enable the estimation of any intrinsic codon–anticodon pairing stabilities. The results presented show that the conception of codon–anticodon pairing as an interaction between solely trinucleotidic sequences is insufficient. With respect to

stabilities, the nucleobases close to the 3'-ends have to be taken into account. Biological phenomena that concern the accuracy of ribosomal translation should, particularly, be newly analysed in terms of their codon context. In this sense, we are extending the current studies towards a systematic comparison of coded and recoded codon-anticodon complexes encountered during ribosomal tRNA slippage, in order to reveal differences in the base-stacking patterns as a determinant for frameshift events.^[15]

Received: November 11, 1999 [Z14255]

- [1] a) B. Alberts, D. Bray, J. Lewis, M. Raff, K. Roberts, J. D. Watson, *Molecular Biology of the Cell*, Garland, New York, **1995**; b) C. M. T. Spahn, K. H. Nierhaus, *Biol. Chem.* **1998**, *379*, 753–772.
- [2] J. H. Cate, M. M. Yusupov, G. Z. Yusupova, T. N. Earnest, H. F. Noller, *Science* **1999**, *285*, 2095–2104.
- [3] a) G. M. Clore, A. M. Gronenborn, L. W. McLaughlin, *J. Mol. Biol.* **1984**, *174*, 163–173; b) G. M. Clore, A. M. Gronenborn, E. A. Piper, L. W. McLaughlin, E. Graeser, J. H. van Boom, *Biochem. J.* **1985**, *221*, 737–751; for codon-anticodon interactions in general, see: c) S. Yoshizawa, D. Fourmy, J. D. Puglisi, *Science* **1999**, *285*, 1722–1725; d) R. C. Morris, K. G. Brown, M. S. Elliott, *J. Biomol. Struct. Dyn.* **1999**, *16*, 757–774; e) V. I. Lim, G. V. Aglyamova, *Biol. Chem.* **1998**, *379*, 773–781; f) D. Smith, M. Yarus, *Proc. Natl. Acad. Sci. USA* **1989**, *86*, 4397–4401.
- [4] W. Saenger, *Principles of Nucleic Acid Structure*, Springer, Berlin, **1984**, pp. 141–149.
- [5] a) E. Westhof, P. Dumas, D. Moras, *Acta Crystallogr. Sect. A* **1988**, *44*, 112–123; b) M. Sprinzl, C. Horn, M. Brown, A. Ioudovitch, S. Steinberg, *Nucleic Acids Res.* **1998**, *26*, 148–153.
- [6] For examples of experimental references to interactions of this kind see: a) D. Ayer, M. Yarus, *Science* **1986**, *231*, 393–395; for theoretical concepts such as “The Hypercycle” see also: b) M. Eigen, P. Schuster, *Naturwissenschaften* **1978**, *65*, 341–369.
- [7] For the natural occurrence and significance of *m*¹*G* see: a) G. R. Björk in *tRNA: Structure, Biosynthesis, and Function* (Eds.: D. Söll, U. RajBhandary), ASM Press, Washington DC, **1995**, pp. 165–205; b) S. Yokoyama, S. Nishimura in *tRNA: Structure, Biosynthesis, and Function* (Eds.: D. Söll, U. RajBhandary), ASM Press, Washington DC, **1995**, pp. 207–223; for the preparation of *m*¹*G* building blocks for automated solid-phase synthesis see: c) M. Sekine, T. Satoh, *J. Org. Chem.* **1991**, *56*, 1224–1227; d) P. F. Agris, A. Malkiewicz, A. Kraszewski, K. Everett, B. Nawrot, E. Sochacka, J. Jankowska, R. Guenther, *Biochimie* **1995**, *77*, 125–134.
- [8] Linkers based on ethylene glycol, tri- and tetrakisethylene glycol phosphate, and 1-hydroxy-propan-3-phosphate were optimized at various length as loop replacements within the hairpin sequences rUGGA-UUUU-UCCAG, rUCCAG-UUUU-UGGA, and rUGGA-UUUU-GUCCA: W. Pils, R. Micura, unpublished results; see also: a) S. Rumney, E. T. Kool, *J. Am. Chem. Soc.* **1995**, *117*, 5635–5646; b) F. Benseler, D.-j. Fu, J. Ludwig, L. W. McLaughlin, *J. Am. Chem. Soc.* **1993**, *115*, 8483–8484; c) A. C. Moses, A. Schepartz, *J. Am. Chem. Soc.* **1997**, *119*, 11591–11597; d) J. P. Bartley, T. Brown, A. N. Lane, *Biochemistry* **1997**, *36*, 14502–14511; e) M. Durant, K. Chevie, M. Chassignol, N. T. Thuong, J. C. Maurizot, *Nucleic Acid. Res.* **1990**, *18*, 6353–6359; f) M. Y.-X. Ma, K. McCallum, S. C. Climie, R. Kuperman, W. C. Lin, M. Sumner-Smith, R. W. Barnett, *Nucleic Acids Res.* **1993**, *21*, 2585–2589.
- [9] tRNA^{Phe} comprising *m*¹*G* (position 37) together with guanosine or 2'-*O*-methylguanosine (position 34) is found in several organisms see: ref. [5b].
- [10] R. Micura, *Chem. Eur. J.* **1999**, *5*, 2077–2082.
- [11] a) L. Markey, K. Breslauer, *Biopolymers* **1987**, *26*, 1601–1620; b) T. Xia, D. H. Mathews, D. H. Turner in *Comprehensive Natural Product Chemistry, Vol. 8* (Eds.: D. Söll, S. Nishimura, P. Moore), Elsevier, Oxford, UK, **1999**, pp. 21–47; c) M. Petersheim, D. H. Turner, *Biochemistry* **1983**, *22*, 256–263.
- [12] P. Strazewski, *Helv. Chem. Acta* **1995**, *78*, 1112–1143.

- [13] Effects of stabilization by tRNA-purine-37 are discussed, but have only been quantified with respect to tRNA/tRNA-dimerizations so far. See: C. Houssier, H. Grosjean, *J. Biomol. Struct. Dyn.* **1985**, *3*, 387–408.
- [14] For the relevance of *m*¹*G* concerning frameshifting see: G. R. Björk, *EMBO J.* **1999**, *18*, 1427–1434.
- [15] a) J. Atkins, R. Gesteland in *tRNA: Structure, Biosynthesis, and Function* (Eds.: D. Söll, U. RajBhandary), ASM Press, Washington DC, **1995**, pp. 471–490; b) R. Gesteland, J. Atkins, *Annu. Rev. Biochem.* **1996**, *65*, 741–768; c) P. Farabaugh, *Annu. Rev. Genet.* **1996**, *30*, 507–528.

A Convenient and General Tin-Free Procedure for Radical Conjugate Addition**

Cyril Ollivier and Philippe Renaud*

Radical reactions are becoming an extremely useful tool in organic synthesis, particularly for the formation of carbon-carbon bonds in intra- and intermolecular processes.^[1] The very rapid development of these reactions could be attributed to the emergence of highly efficient ways to conduct them. Among these methods, the tin hydride mediated addition of radicals to activated alkenes has played a major role.^[2] However, the application of this reaction for the synthesis of pharmaceuticals is severely limited by the toxicity of the tin reagents and by the difficulty in removing traces of organotin residues from the final products. Therefore, alternative ways of running radical reactions are under intensive investigation.^[3] Recently, we have reported a modified version of the Brown-Negishi reaction^[4] where efficient hydroborations with catecholborane and radical additions to enones and enals were performed in a one-pot procedure (Scheme 1).^[5a] This oxygen-initiated reaction proved to be efficient with enones and enals. However, other classical radical traps such as unsaturated esters, amides, and sulfones failed to react. Herein, we present an efficient procedure to run one-pot hydroboration for radical addition to any kind of activated alkenes. The reaction is based on the use of a Barton carbonate as radical chain transfer reagent (RCTR).^[6]

The failure of our modified version of the Brown-Negishi reaction with classical radical traps such as acrylate moieties was interpreted as a consequence of an inefficient propagation step resulting from the reaction between the radical adducts and *B*-alkylcatecholboranes. This inefficiency is caused by the lower density of unpaired electrons at the

*] Prof. P. Renaud, C. Ollivier
Université de Fribourg
Institut de Chimie Organique
Pérolles, 1700 Fribourg (Switzerland)
Fax: (+41) 26-300-9739
E-mail: philippe.renaud@unifr.ch

**] Organoboranes in Radical Reactions. Part 4. This work was generously supported by the Fonds National Suisse de la Recherche Scientifique. We thank Valéry Weber for performing some preliminary experiments. Parts 1–3: see ref. [5].